Journal of Fluorescence (2019) 29:1301–1309
https://doi.org/10.1007/s10895-019-02445-6

ORIGINAL ARTICLE

Spectroscopic Properties of some Hydroxylated 2-Stilbazole Derivatives

Alexander V. Semenov[1] · Olga I. Balakireva[1] · Irina V. Tarasova[1] · Elena V. Semenova[2] · Olga V. Minaeva[2]

Received: 5 July 2019 / Accepted: 23 September 2019 / Published online: 12 November 2019

Abstract

The spectroscopic properties for a number of new hydroxylated 2-stilbazoles were studied by absorption and fluorescence spectroscopy. The maximum absorption and emission wavelengths, the molar extinction coefficients, and the Stokes shift values of derivatives were given. The dependence of the spectral characteristics on pH was shown. The possibility of creating molecular logic systems and fluorescent dyes for bioimaging based on these derivatives was demonstrated. The dependence of fluorescence on the medium redox properties was established for an one of derivatives. The possibility of a fluorescent probe creating on its basis to assess the oxidative state of living systems was demonstrated. The probe has good biocompatibility and can be successfully used for fluorescence imaging in cells.

Keywords 2-Stilbazoles · Photophysical properties · Fluorescent probe · Cell imaging · Logic gate

Introduction

The stilbene heterocyclic analogues have attracted the attention of researchers for a long time as a structural basis for fluorescent materials with pronounced photophysical and electro-optical properties [1]. In particular, isomeric styrylpyridines - stilbazoles are objects of interest. It was established that the luminescence spectra of unsubstituted isomeric stilbazoles are similar to stilbene spectra. At the same time, the stilbazoles excited states are unlike those for stilbenes, due to they have nπ* state in addition to stilbene energy levels. In this case, the nπ* state effect strongly depends on the styryl fragment position. It is involved in charge transfer from the pyridine cycle to the benzene ring in 2- and 4-isomers, but its effect is limited only by the pyridine cycle in the 3-isomer. In addition, stilbazoles, unlike stilbenes, have a significant permanent electric dipole moment, are capable of forming a new conformational equilibrium (rotational isomerism), and in some cases the weak intramolecular hydrogen bonds [2]. Conformational isomers of the ground state arising from the lack of aryl groups' free rotation around a quasi-simple bond with an ethylene bridge can have dissimilar radiative and nonradiative decay parameters in an excited state. These aspects change the spectroscopic, photophysical and photochemical properties of aza-derivatives in comparison to the initial hydrocarbons.

A study of the stilabazoles' fluorescence spectra shows their strong dependence on pH and solvent polarity [3]. Usually, the pyridine fragment protonation is accompanied by a bathochromic shift of the maximum luminescence. A red shift is also observed in a more polar medium.

The low-energy nπ* state in unsubstituted stilbazoles promotes the emergence of new non-radiative paths to deactivate the excited state. As a result, the stilbazoles luminescence spectra characterize by lower signal intensity than stilbenes. The quantum yield of fluorescence is $\varphi_{fl} = 0.07$ for the 3-isomer, which is twice as large as stilbene ($\varphi_{fl} = 0.035$ [4]), but it falls to $\varphi_{fl} = 0.003$ and 0.005 for 2- and 4-isomers, respectively [1].

The introduction of a hydroxyl group, which has a pronounced electron-donor effect, into the stilbazole molecule has a significant effect on the electron density distribution in the conjugated system. It also creates the possibility of anionic structure and zwitterionic phototautomer formation in the

Electronic supplementary material The online version of this article (https://doi.org/10.1007/s10895-019-02445-6) contains supplementary material, which is available to authorized users.

✉ Alexander V. Semenov
salexan@mail.ru

[1] Physics and Chemistry Institute, National Research Mordovia State University, 68 Bolshevistskaya str, 430005 Saransk, Russia

[2] Medicine Institute, National Research Mordovia State University, 26A Ul'yanova str, 430032 Saransk, Russia

excited state along with the neutral and cationic forms [3] thereby expanding the number of forms involved in absorption and fluorescence (Scheme 1).

Structures of this type are interesting as fluorescent chemosensors for pH determination [5]. In addition, pH-sensitive molecular systems exhibiting fluorescent properties have been proposed for building controlled photo switches and molecular logic devices based on them [6]. The implementation of logical functions with ion-, electro-, or photo-switching molecules is at the center of research related to the growing need for further miniaturization in information technology. Currently, the main logic elements using in a conventional silicon circuit can be simulated at the molecular level by chemical or optical signals. The mathematical calculations require the joint operation of several fundamental gates, so the rational integration variants of elementary logic gates into high-level circuits, especially within one simple molecule, become especially interesting.

Fluorogenic antioxidants-indicators also attract the researchers' attention as potential non-invasive systems of spatial and temporal monitoring of the oxidation state in a living cell at the organelle level in order to better understanding the vital links between chemistry and ROS biology [7].

Previously, we synthesized a number of new hydroxylated 2-stibazoles with the general structure (**2**) (Fig. 1) and investigated their antioxidant properties [8].

The wide range of potential applications of the hydroxylated stilbazoles' fluorescent effects prompted us to investigate the photophysical properties of the derivatives (**2**).

Experimental

Materials

All reagents and solvents in spectroscopic studies purchased from commercial suppliers had the analytical grade and used without further purification. The compounds **2a-e** were synthesized according to previously described methods [8].

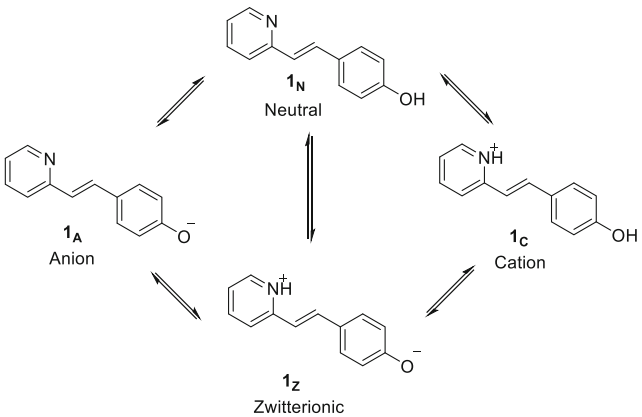

Scheme 1 Molecular structures of the neutral ($\mathbf{1_N}$), anionic ($\mathbf{1_A}$), cationic ($\mathbf{1_C}$) and zwitterionic ($\mathbf{1_Z}$) states of **1**

Methods and Instrumentation

Photophysical Properties

The UV-VIS absorption spectra were measured by an UV-2600 recording spectrophotometer (Shimadzu, Tokyo, Japan). Fluorescence spectra were recorded using an RF-5301 PC spectrofluorophotometer (Shimadzu, Tokyo, Japan). All spectra were recorded at room temperature. The emission spectra were corrected and the solvent background was subtracted.

Fluorescence quantum yields were determined from the fluorescence spectrum using the value of absorption peak at 285 nm $\varphi_{ref} = 0.60 \pm 0.05$ [9] for 2-aminopyridine in 0.05 M H_2SO_4 as a reference. The determination of fluorescence quantum yields was carried out according to [10]. The calculated quantum yields were adjusted for differences in the absorption peak and solvents refractive index. The values presented are calculated as the average of three measurements, with errors determined by the maximum spread between the experimental data.

The pH measurements were carried out at room temperature using the pH electrode ES-10603/7 on the pX-150MI ion meter (Russia). The reference buffer solutions were used for the electrode system calibration.

Cell Culture and Fluorescence Imaging

The study was carried out on a cell culture of mouse L929 fibroblasts (obtained from the Tissue Culture Collection of the Ivanovsky Virology Research Institute). After defrosting, the cells were cultured in vials on DMEM medium (PanEko, Russia) with the addition of 10% fetal calf serum (HyClone, USA) under standard conditions (5% CO_2, 37°C, 5% wetness; Sanyo incubator, Japan).

In the experiment, the cells were placed on a sterile cover glass at the wells bottom of a 6-hole tablet at $2 \cdot 10^4$ cells/well in 500 μl of the medium, after the cells had settled and attached to the glass, another 1.5 ml of DMEM medium with 10% FBS was carefully added. The plates were incubated for 24 h. Immediately before the experiment, the medium was removed, a solution of the studied substances in a physiological solution at a concentration (20 μM) in a volume of 1 ml was added to the wells in a monolayer, and 1 ml of NaCl 0.9% was used as a control. The plates were covered with foil and placed in an incubator.

Fluorescence microscopy of the samples was carried out immediately after application (point 0′) and in dynamics after 5, 10, 15, 30 min, 1 and 2 h. A fresh sample was used for each time point. Microscopic research was performed directly in the well of the tablet under a cover glass on a fluorescent microscope

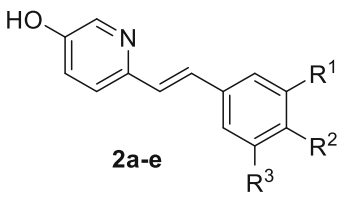

	R1	R2	R3
a	H	H	H
b	H	OH	H
c	OH	OH	H
d	OH	H	OH
e	OH	OH	OH

Fig. 1 Structures of the investigated compounds

(Axio zeiss imager a2, Carl Zeiss, Germany) using a 1.2 NA 63x water objective. Cells were imaged using a DAPI filter cube (352-402 nm excitation, 417-477 nm emission).

Results and Discussion

Absorption and Emission Studies

The study of adsorption and emission characteristics for hydroxylated stilbazoles (**2a-e**) was carried out in neutral ethanol and in a solvent with the addition of 0.1 M HCl and 0.1 M KOH. UV data: maximum absorption wavelength (λ_{max}) and molar extinction coefficient (ε), as well as fluorescence characteristics: maximum fluorescence (λ_{em}), Stokes shift ($\Delta\lambda$) and quantum fluorescence yield (φ_f) in all solvents used, summarized in Table 1.

Ultraviolet Absorbance Spectra

Hydroxy substituted stibazoles under neutral conditions in ethanol (Table 1, Fig. 2) generally show the similar spectra having an absorption band with a maximum of about 330 nm. At the same time, a red shift is clearly visible in the hydroxyl group presence in the 4-th position of the benzene ring (compounds **2b**, **2c** and **2e**). The shifts reach maximum values with the simultaneous presence of hydroxyl group in position 3 (compounds **2c** and **2e**). The more pronounced shoulder appears in the shortwave region of compounds **2a–d** spectra. The maximum molar extinction coefficients are observed for **2a** and **2b**, they are 3.07×10^4 $Lmol^{-1}$ cm^{-1} and 2.98×10^4 $Lmol^{-1}$ cm^{-1}, respectively.

The absorption intensity somewhat decreases under acidic or basic conditions. Two new bands appear in an acidic medium in the intervals of 300–310 nm and 340–390 nm, respectively. Moreover, the longer wavelength band has a greater intensity. In the basic medium, the studied compounds show a new long-wavelength absorption band. However, it should be noted that the absorption spectra for compounds **2c** and **2e** in an alkaline medium differ significantly from other derivatives. Probably the reason for this phenomenon is the degradation process of these compounds, mentioned in [11] for related systems containing a catechol fragment. This

Table 1 Estimated photophysical properties of compounds **1** and **2a-e**

Compound	Conditions	λ_{max}, nm	$\varepsilon \times 10^{-4}$, $Lmol^{-1}$ cm^{-1}	λ_{em}, nm	$\Delta\lambda$	φ_f
1[a]	Neutral	330	2.30	409	79	0.003[b]
	Acidic	382	2.52	510	128	
	Basic	376	3.29	511	135	
2a	Neutral	318	3.07	378	60	0.140
	Acidic	346	1.75	427	81	0.014
		300	1.16	365	65	0.090
	Basic	330	1.79	438	108	0.023
2b	Neutral	329	2.98	411	83	0.014
	Acidic	369	1.58	496	127	0.007
	Basic	352	2.32	432	80	0.010
2c	Neutral	337	2.94	426	89	0.029
	Acidic	305	1.16	362	57	0.037
		385	2.66	497	112	0.002
	Basic	317	1.80	535	218	0.065
		463	1.26	534	91	0.162
2d	Neutral	322	2.44	423	101	0.020
	Acidic	356	2.24	401	55	0.003
		310	1.32	362	52	0.059
	Basic	346	2.58	410	64	0.005
2e	Neutral	337	2.54	430	93	0.019
	Acidic	303	0.95	370	67	0.008
		390	2.23	516	126	0.001
	Basic	381	0.91	488	107	0.003

[a] Data of [3]. [b] Data of [1]

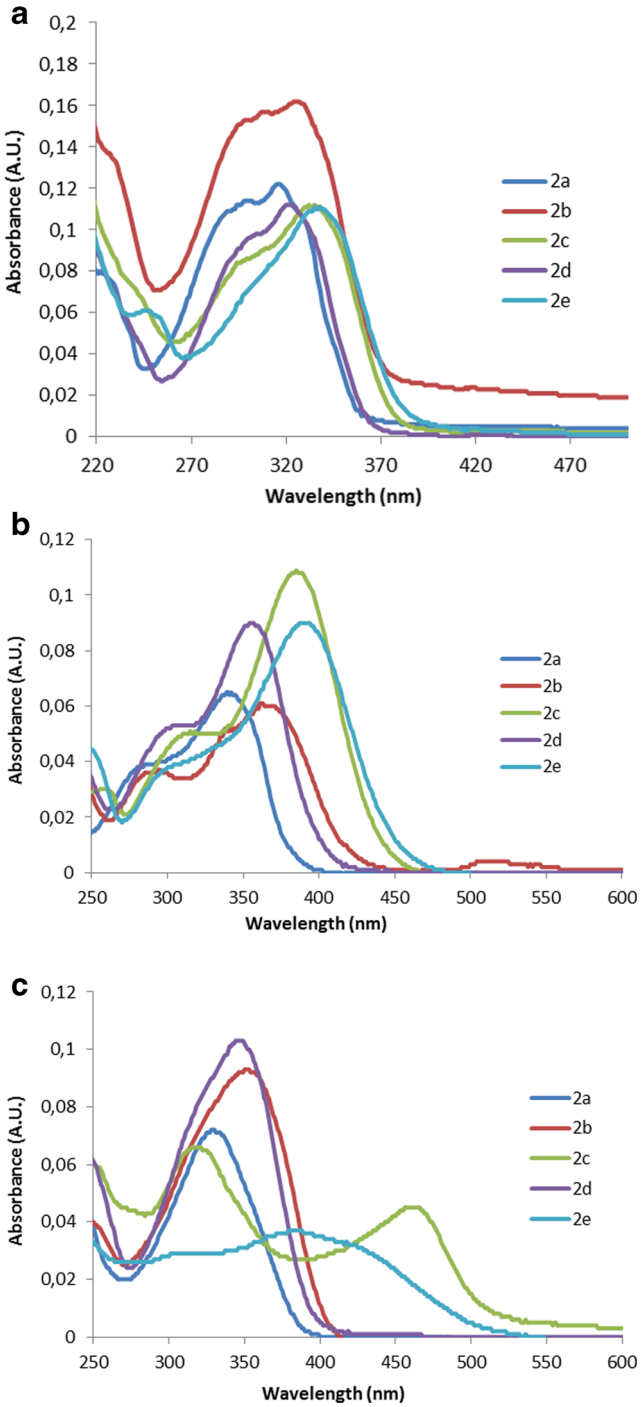

Fig. 2 UV-vis spectra for compounds **2a-e**: (4 μM in ethanol): neutral (**a**), acidic (**b**) and basic (**c**) conditions

statement can be confirmed by the time-dependent changes in the ^{1}H and ^{13}C NMR spectra of compound **2c** in the methanol solution with KOH presence (see Fig. S16 and S17 in the Supporting Information). At first, the base addition leads to only the chemical shifts change in the NMR spectra without the changing of the signals' number and multiplicity. This is probably due to the formation of the anionic form of compound **2c**. However, over time, changes become more dramatic and ultimately there is complete degradation of the native structure. It is important to note that the process of interconversion of various ionized forms of compounds **2** is completely reversible in all other cases, which proves the reduction of the original absorption spectra when the corresponding pH of the medium is returned.

Fluorescence Spectra

It can be summarize the several regularities about the fluorescent radiation of hydroxy-substituted molecules. The radiation and intensity maxima show a strong dependence on the medium pH in all cases: a pronounced red shift is observed during the transition from neutral to acidic or basic conditions. So, if in a neutral medium the emission occurs in the range of 378–430 nm, in the basic medium emission band, as a rule, are shifted to 438–535 nm, in the acidic medium - to 427–516 nm (Fig. 3). The double emission was observed for compounds **2c-2e** in some cases (mainly in acidic conditions).

To determine the fluorescence efficiency, quantum outputs were calculated (the values are given in Table 1). It was found that the hydroxyl group introduction in the 3-position of the pyridine ring leads to quantum yield increasing by about an order of magnitude (compare compounds **1** and **2**). The maximum value was observed for compound **2a**. At the same time, the introduction of the hydroxyl groups in the benzene fragment (especially in position 4) led to a slight fluorescence intensity decreasing. It was found that the nitrogen atom protonation or the hydroxyl groups deprotonation contributed to quantum yield decreasing in most cases. The exception was the compound **2c**: there was a marked fluorescence intensity increasing and a significant difference in the emission band in comparison to other derivatives in an alkaline medium. This fact also indicates the process of compound's structure degradation in a strongly alkaline medium.

Dependence of Absorption and Emission Spectra of Compound 2c on pH

The specific behavior of compound 2c is the reason for the more detail studying of the depend-ence of its absorption and emission spectra on pH changes. As reported in [11] and observed by changes in NMR spectra, probably, the polymerization of the stilbazoles containing a catechol frag-ment occurs in strongly alkaline medium. At the same time, the fact of diphenols autooxidation to the corresponding ortho-quinones at pH > 7.5 is well known. So, there is a prospect of using of the observed changes to monitor the oxidation state in living systems.

We have carried out a series of experiments in the aqua medium. The standard phosphate (PB) and borate (BB) buffer systems were used to maintain pH. The absorption spectra of compound **2c** at different pH values are presented in Fig. 4.

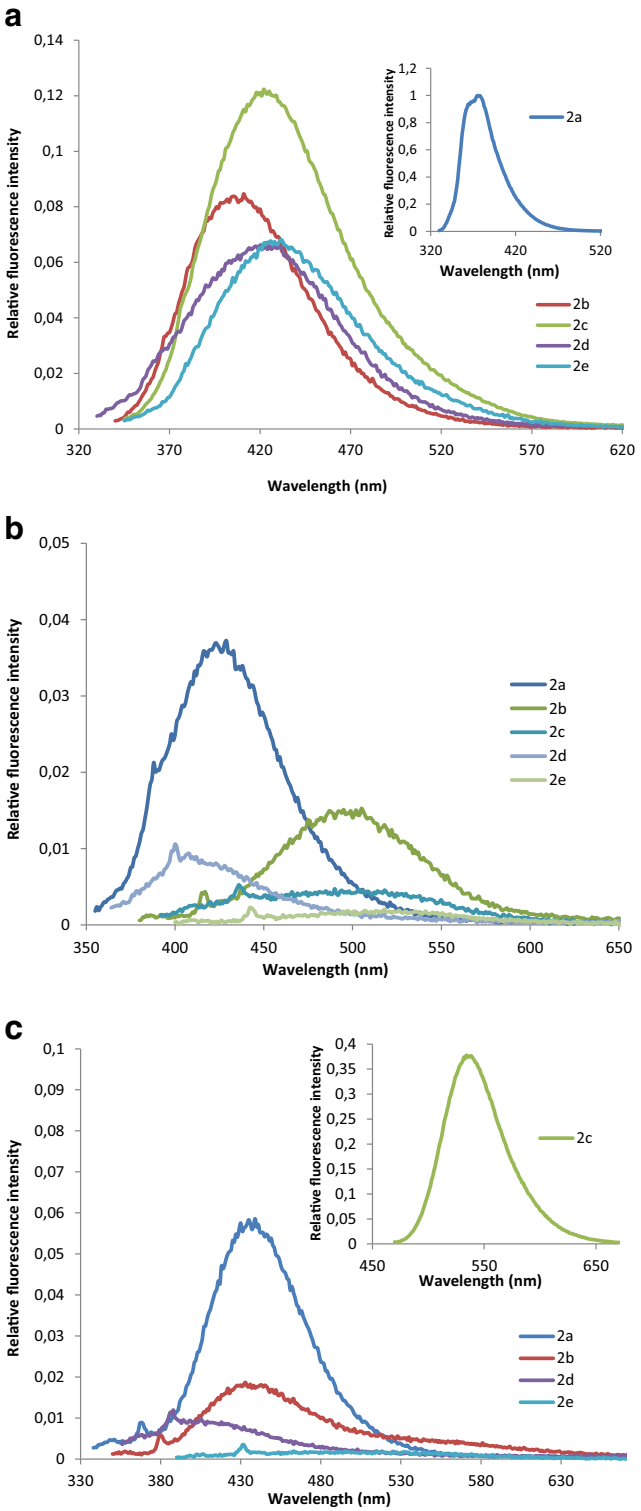

Fig. 3 Comparative normalized emission spectra of synthesized derivatives **2a-e** (4 μM in ethanol): neutral (**a**), acidic (**b**) and basic (**c**) conditions

In a neutral medium, both in degassed distilled water and in the corresponding buffer systems, identical absorption spectra are observed with a maximum at 330 nm and a shoulder in a shorter wavelength region. The maximum's shift to a longer wavelength region with general retention of the peak shape is observed upon transition to an acidic medium. This process can be controlled and reversibly shifted forward or backward through acid-base titration.

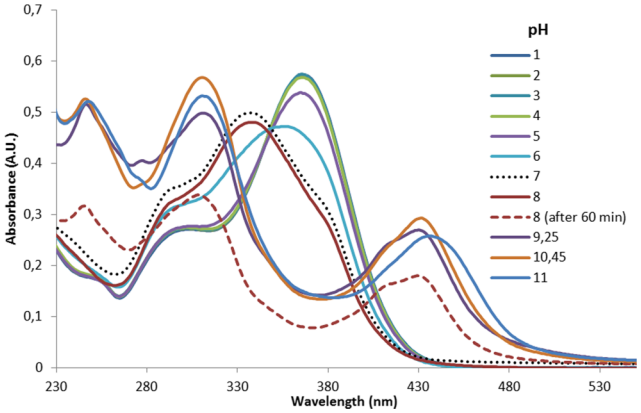

Fig. 4 UV-vis spectra for compound **2c** (25 μM in PB) at different pH values

At pH ≥7.5, the original spectrum shape remained similar to that for a neutral medium with a small bathochromic shift of the absorption maximum. However, the nature of the spectrum changed dramatically over time, and two new absorption maxima were observed in the 300 nm and 430 nm regions. The absorption in the region of 400–450 nm and the appearance of yellowish color of solutions are characteristic for ortho-quinones. The rate of this change increased significantly with the transition to higher pH values. It is interesting to note that the changing process was longer in the alkaline region (see Fig. 5), and the color appearance was not observed after replacing the phosphate to borate buffer system at the same pH values.

Probably, this fact can be explained by the catechol fragment interaction with boric acid in an alkaline medium, which leads to the formation of a reversible catechol-

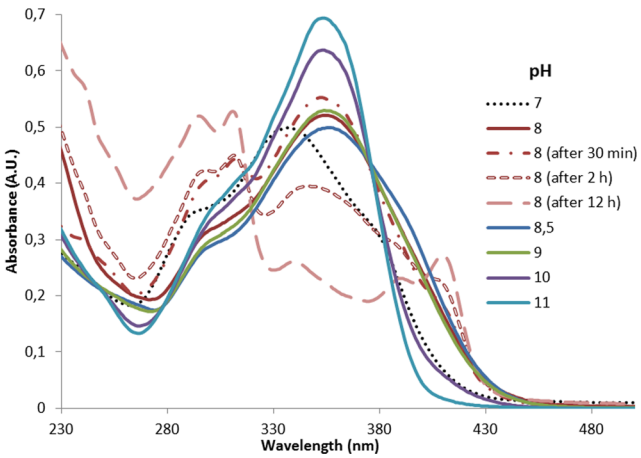

Fig. 5 UV-vis spectra for compound **2c** (25 μM in BB) at different pH values

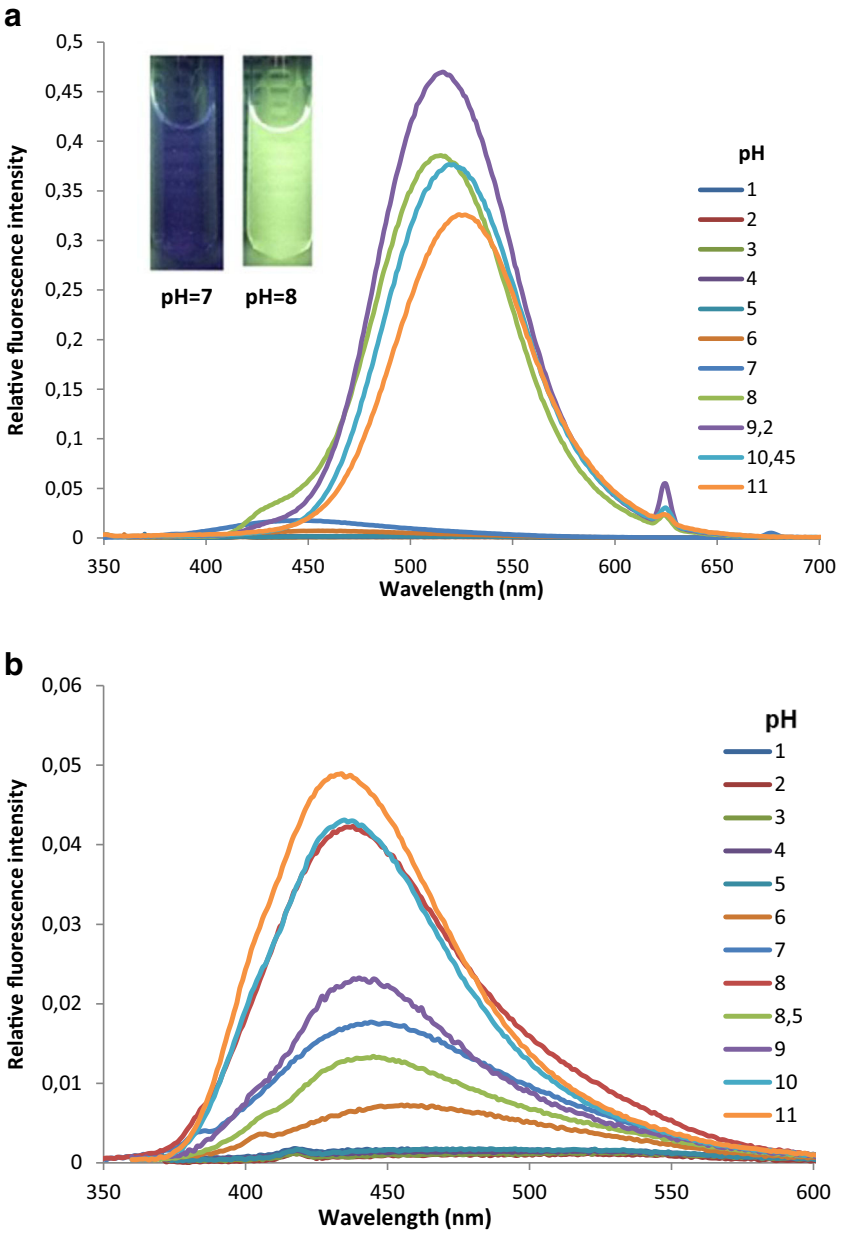

Fig. 6 Comparative normalized emission spectra of **2c** (4 μM) in PB (**a**) and BB (**b**) at different pH values

borate complex, partially protecting the compound from further oxidation [12].

Confirmation of this phenomenon can be found in the fluorescence spectra studying. It has been established that fluorescence intensity drops significantly without a significant change in its maximum during the transition from a neutral to an acidic medium. At the same time, the sharp fluorescence intensity increasing occurs with the maximum's shift to the green area in the media with pH ≥ 7.5. The process is significantly accelerated with increasing pH. The fluorescence maximum remains in the blue region of the spectrum, and its intensity doesn't increase as dramatically in the borate buffer (see Fig. 6).

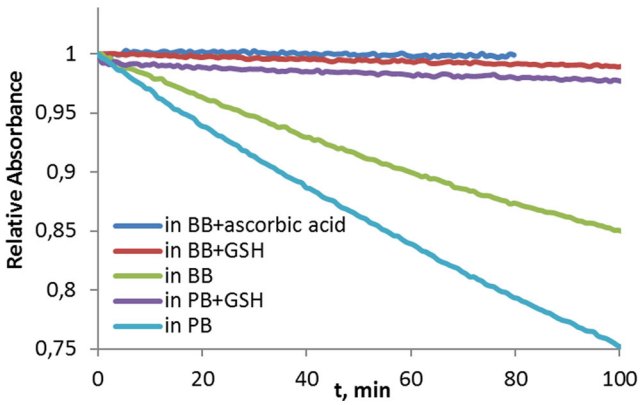

Fig. 7 Time-dependent changes of absorbance intensities at 330 nm for **2c** at pH 8

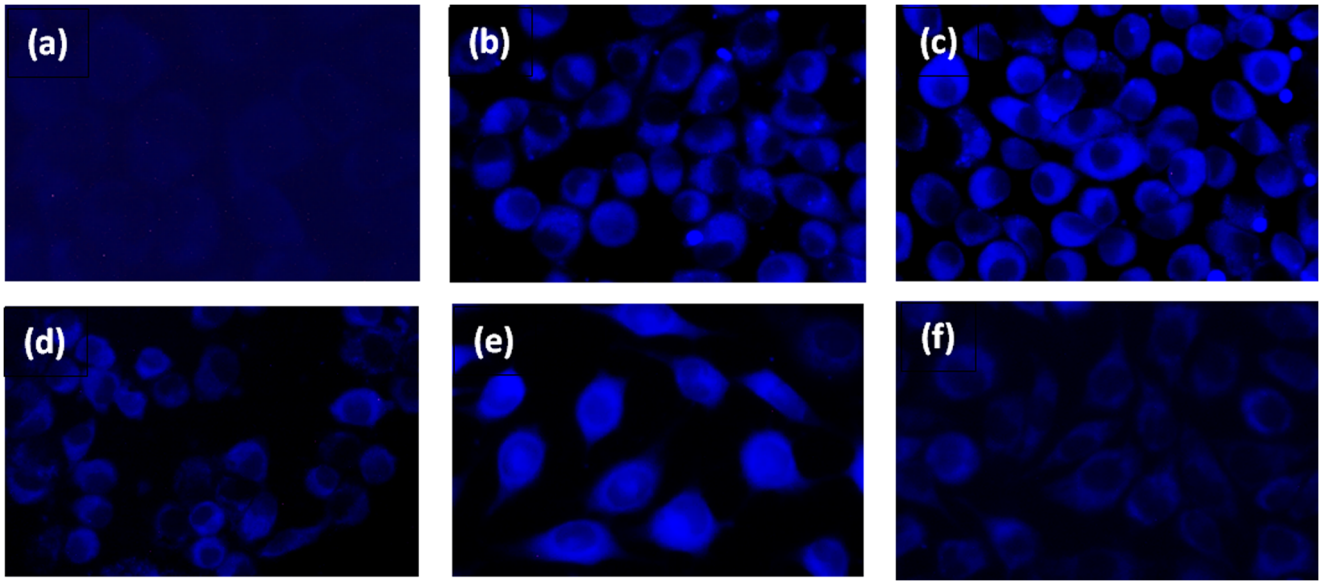

Fig. 8 Fluorescence images of fibroblast cells no additive (**a**), containing **2a** (**b**), **2b** (**c**), **2c** (**d**), **2d** (**e**), **2e** (**f**)

Thus, the probable reason for intense fluorescence in an alkaline medium is the formation of ortho-quinone and/or its further degradation products.

To assess the possibility of using the observed processes in the study of the oxidative state of living systems, we evaluated the glutathione effect on the formation of intensely fluorescent products of the oxidative degradation of compound **2c**. It is known that this dipeptide largely determines the redox characteristics of the intracellular medium, and the ratio of reduced and oxidized forms of glutathione in the cell is one of the most important parameters indicating the oxidative stress level [13].

Comparison of the oxidative degradation rates showed that the process in the borate buffer occurs on average twice slower than in the phosphate buffer (Fig. 7). The oxidative degradation process of compound **2c** slows down dramatically in both borate and phosphate buffer systems at the presence of a reduced form of glutathione (GSH), which prevents the formation of intensely fluorescent products (see Fig. 6). A similar effect was observed with using another natural antioxidant - ascorbic acid. Thus, compound **2c** can be considered as a new tool to study redox chemistry in biological systems.

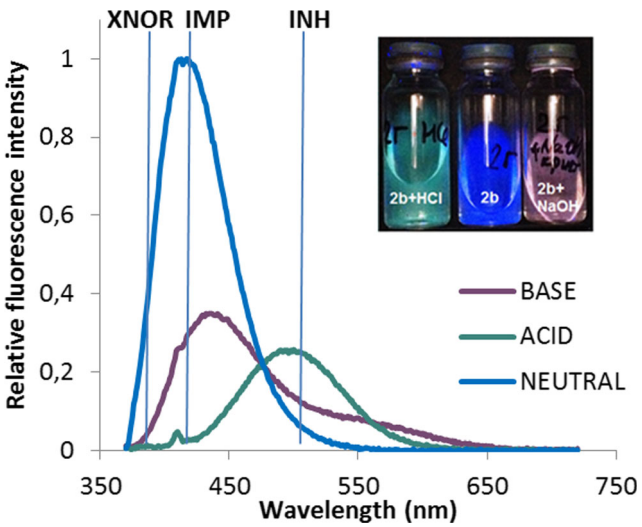

Fig. 9 Fluorescence spectra and fluorescence color changes for **2b** in different mediums

Bio-Imaging Experiments on Fibroblasts

In order to use the prepared compounds in biological applications, we investigated their cytotoxicity in a previous paper [8]. According to the results, compounds **2** demonstrated low cytotoxicity.

The low toxicity of the compounds and the presence of UV fluorescence in the visible region prompted us to bio-imaging experiments. The cells incubated with compounds **2** in comparison with control cells were investigated. The fluorescence imaging of fibroblast cells shows on Fig. 8.

Table 2 Set of truth tables showing superposed logic gates for **2b**

Input		Output A		Output B	Output C
Acid	Base	λ = 390 нм		λ = 415 нм	λ = 500 нм
		Positive logic	Negative logic		
0	0	1 (0.49)	0 (0.49)	1 (0.99)	0 (0.08)
1	0	0 (0.01)	1(0.01)	0(0.02)	1 (0.26)
0	1	0 (0.06)	1(0.06)	1 (0.27)	0 (0.14)
1	1	1 (0.49)	0 (0.49)	1(0.99)	0 (0.08)
Logic functions		XNOR	XOR	IMP	INH

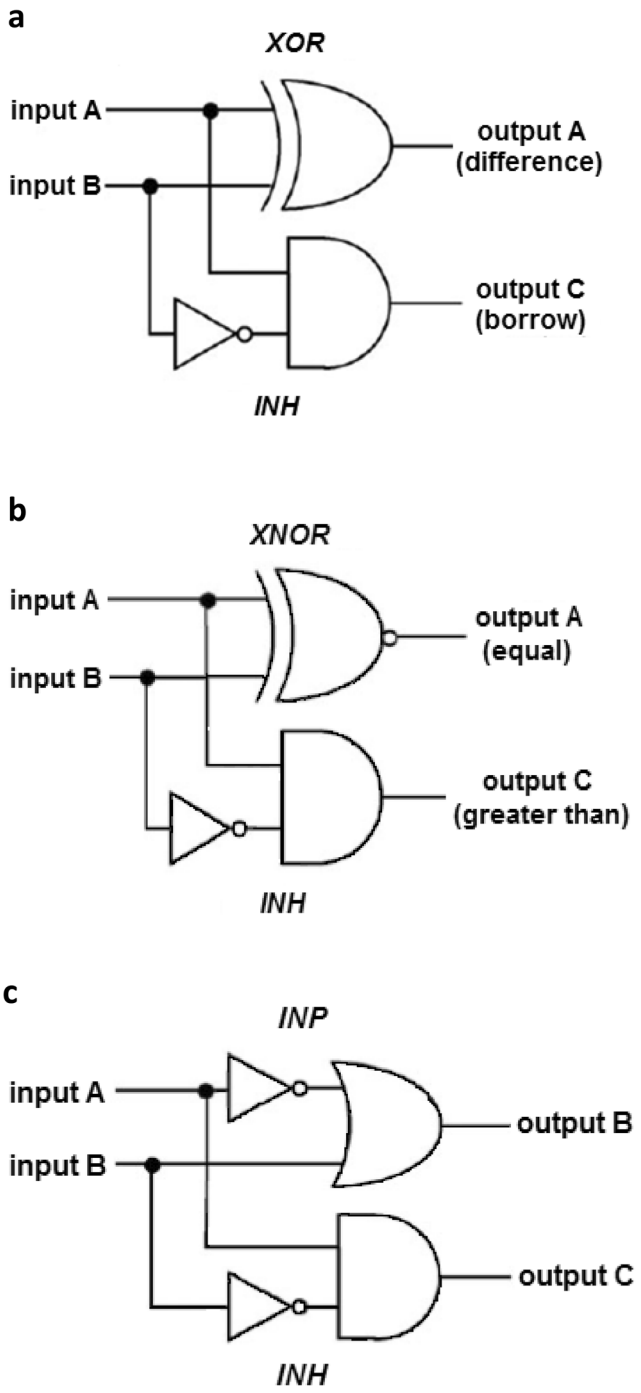

Fig. 10 Circuit diagrams for half-subtractor (**a**), magnitude comparator (**b**) and a complementary output IMP/INH (**c**)

These data indicate that all testing compounds are able to penetrate into the fibroblasts and produce the intense blue fluorescence in most cases, while control cells didn't show significant fluorescence. Thus, the test substances are able to interact with fibroblast cells without harming or killing them.

The series of time-dependent fluorescence signals (images were recorded after 0 min, 10 min, 30 min, 60 min, and 120 min, respectively) of fibroblasts stained with compounds **2** showed that the maximum fluorescence is reached by about 30 min and remains relatively stable (see Fig. S11-S15). It is noteworthy that the compounds penetrate differently into the cytoplasm and fibroblast nucleolus.

The difference between the fluorescent radiation of cytoplasm and the nucleus is clearly visible in Fig. 3c. This feature of the luminescent pattern, and sufficiently high-quality images of cells, especially those obtained by incubation with compound **2b**, open up prospects for the compounds' using in single- or multi-color bioimaging.

Logic Gate Application

It is possible to build the logical systems based on the dependence of the fluorescence of compounds **2** on the pH and the reversibility of this transition. In these systems, solutions of compounds **2** play the role of a logical element, while acid and base are used as an input signal and fluorescence as an output signal. The presence and absence of input signals was defined as 1 and 0, respectively. The molecular logic systems actually have a single output signal for the majority of the compounds studied. Therefore, these systems are capable of performing one logical operation (XNOR gate with positive or XOR with negative logic, see Appendix). But for the compound **2b** can be developed several combinatorial logic systems based on pH-mediated multi-signal response by rational determination of logical states.

The Fig. 9 and Table 2 show the possibility of forming the logic gates of the INHIBIT logic gate (output 500 nm), IMPLICATION (output 415 nm) and XNOR (output 390 nm) based on the compound **2b**. It is perfectly acceptable to start one channel in positive logic when using negative logic at the output of another channel, due to the assignment of logical polarity (logical 0 and 1) to the inputs and outputs is arbitrary and the logic gates are independent of each other. Thus, following this procedure, the XNOR gate is effectively converted to an XOR gate to exit at 412 nm.

This combination of logic gates allows to construct several logic devices: a simple 1-bit magnitude comparator (in the case of positive logic) or half subtractor (in the case of negative logic.), as well as complementary IMP / INH logic functions. Their schemes are presented in Fig. 10.

Conclusion

Summarizing this research, it is possible to note the high potential of the studied structures for the creating of molecular logic systems and fluorescent dyes for bio-imaging, and especially for developing effective molecular probes for assessing the redox state of biological systems.

References

1. Lipunova GN, Nosova EV, Trashakhova TV, Charushin VN (2011) Azinylarylethenes: synthesis and photophysical and photochemical properties. Russ Chem Rev 80:1115–1133. https://doi.org/10.1070/RC2011v080n11ABEH004234
2. Baraldi I, Spalletti A, Vanossi D (2003) Rotamerism and electronic spectra of aza-derivatives of stilbene and diphenylbutadiene. A combined experimental and theoretical study. Spectrochim Acta A 59:75–86. https://doi.org/10.1016/S1386-1425(02)00117-8
3. Haroutounian SA, Katzenellenboge JA (1988) Hydroxystilbazoles and hydroxyazaphenanthrenes: photocyclization and fluorescence studies. Photochem Photobiol 47:503–516. https://doi.org/10.1111/j.1751-1097.1988.tb08838.x
4. Waldeck DH (1991) Photoisomerization dynamics of stilbenes. Chem Rev 91:415–436. https://doi.org/10.1021/cr00003a007
5. Han J, Burgess K (2010) Fluorescent indicators for intracellular pH. Chem Rev 110:2709–2728. https://doi.org/10.1021/cr900249z
6. Budyka MF (2017) Molecular switches and logic gates for information processing, the bottom-up strategy: from silicon to carbon, from molecules to supermolecules. Russ Chem Rev 86:181–210. https://doi.org/10.1070/RCR4657
7. Krumova K, Cosa G (2013) Fluorogenic probes for imaging reactive oxygen species. Photochemistry 41:279–301. https://doi.org/10.1039/9781849737722-00279
8. Semenov AV, Balakireva OI, Tarasova IV, Burtasov AA, Semenova EV, Petrov PS, Minaeva OV, Pyataev NA (2018) Synthesis, theoretical, and experimental study of radical scavenging activity of 3-pyridinol containing trans-resveratrol analogs. Med Chem Res 27:1298–1308. https://doi.org/10.1007/s00044-018-2150-8
9. Brouwer AM (2011) Standards for photoluminescence quantum yield measurements in solution (IUPAC technical report). Pure Appl Chem 83:2213–2228. https://doi.org/10.1351/PAC-REP-10-09-31
10. Würth C, Grabolle M, Pauli J, Spieles M, Resch-Genger U (2013) Relative and absolute determination of fluorescence quantum yields of transparent samples. Nat Protoc 8:1535–1550. https://doi.org/10.1038/nprot.2013.087
11. Evangelio E, Hernando J, Imaz I, Bardají GG, Alibés R, Busqué F, Ruiz-Molina D (2008) Catechol derivatives as fluorescent Chemosensors for wide-range pH detection. Chem Eur J 14:9754–9763. https://doi.org/10.1002/chem.200800722
12. Kan Y, Danner EW, Israelachvili JN, Chen Y, Waite JH (2014) Boronate complex formation with Dopa containing mussel adhesive protein retards pH-induced oxidation and enables adhesion to mica. PLoS One 9:e108869. https://doi.org/10.1371/journal.pone.0108869
13. Kannan N, Nguyen LV, Makarem M, Dong Y, Shih K, Eirew P, Raouf A, Emerman JT, Eaves CJ (2014) Glutathione-dependent and -independent oxidative stress-control mechanisms distinguish normal human mammary epithelial cell subsets. Proc Natl Acad Sci U S A 111:7789–7794. https://doi.org/10.1073/pnas.1403813111